CHAPTER 3

LITERATURE REVIEW

3.1 INTRODUCTION

Having now established some background about the operational transresistance amplifier, let us turn our attention to discuss some applications of OTRA. OTRA is one of the most important building block in the field of analogue integrated circuit. It can be used to realize different applications such as: differential integrator, differential amplifier, voltage gain amplifiers (VGAs), filters, proportional integral and derivative (PID) controllers, analogue multiplier, immitance simulators, oscillators and square/triangular waveform generator [45-89]. The input terminals of the OTRA are virtually grounded, in consequence, most of the parasitic capacitances and resistances will be disappeared. Then it is possible to obtain accurate transfer function by using OTRA in a negative feedback loop. By using OTRA, it is possible to design the applications without linear passive resistances and it is a known fact, the resistance occupies the large silicon area. The OTRA based applications like filters, differential integrator, differential amplifier and VGAs are implemented without using the passive linear resistors.

3.2 OTRA APPLICATIONS

3.2.1 DIFFERENTIAL AMPLIFIER USING OTRA

The differential amplifier using OTRA [31] with three resistors is shown in Fig. 3.1. This differential amplifier is also called as voltage controlled voltage source (VCVS).

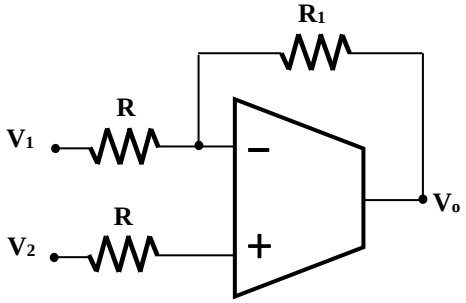

Fig. 3.1 Differential amplifier using OTRA

The output voltage of the differential amplifier circuit shown in Fig. 3.1 is given by

$$V_0 = K(V_2 - V_1) \tag{3.1}$$

where

$$K = \frac{R_1}{R}$$

The circuit in Fig. 3.1 has the advantage of providing equal gain for both inverting and non-inverting inputs, which is independent of bandwidth.

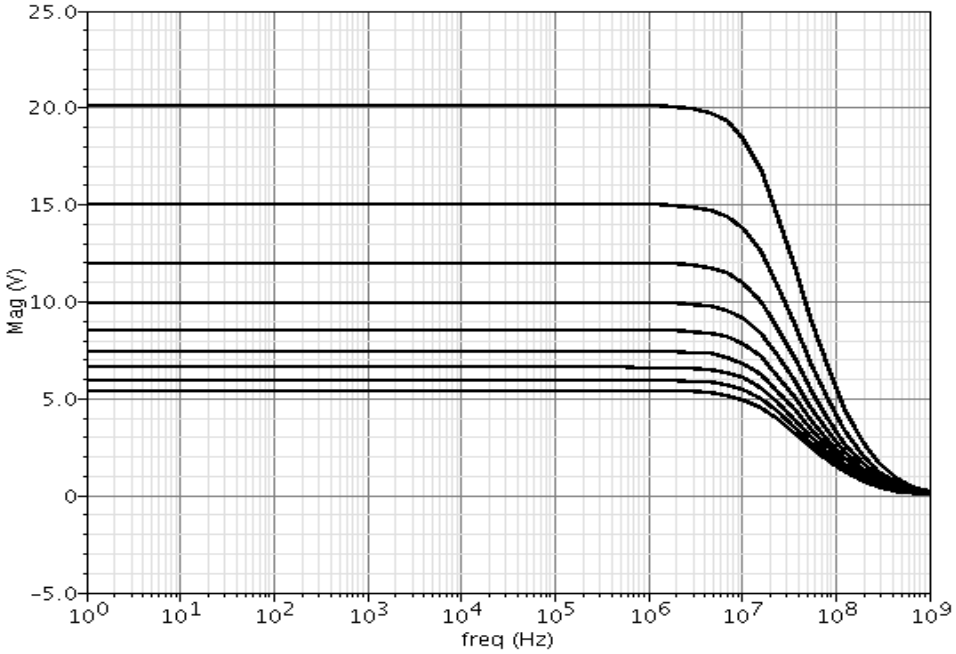

Fig. 3.2 Frequency response of the differential amplifier

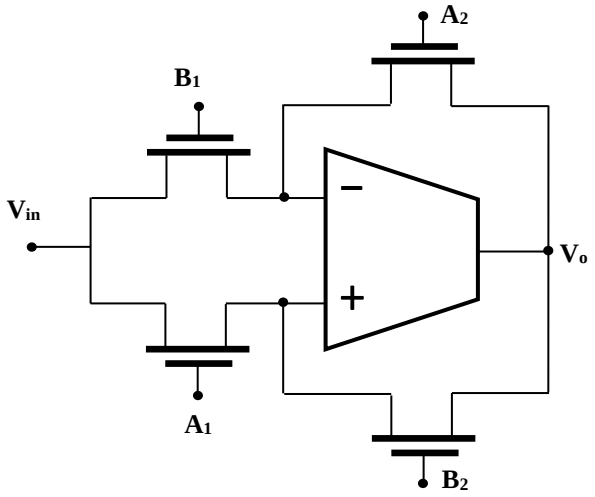

Fig. 3.3 Implementation of differential amplifier using MOS-C [31]

This property is unavailable in traditional voltage-mode (op-amp) devices. The Fig. 3.2 shows the simulation results of the circuit depicted in Fig. 3.1. The passive component values used for the simulation are R_1 is kept constant and R is varied from 1 kΩ to 10 kΩ. The circuit in Fig. 3.1 can also be implemented without using the resistors. The circuit shown in Fig. 3.3 was introduced in [31]. In this work, the application of the OTRA is implemented using MOS-resistors with the non-linearity cancellation technique. The controlled voltage applied to the gate terminal of the transistors can be used to control the conductance G. This implementation is also called as MOS-C (MOSFET and capacitors) implementation. The output voltage at V_o terminal is given by:

$$V_o = (G_1/G_2)V_i \tag{3.2}$$

where

$$G_1 = K_{N1}(V_{A1} - V_{B1}) \tag{3.3}$$

and

$$G_2 = K_{N2}(V_{A2} - V_{B2}) \tag{3.4}$$

$$K_N = \mu C_{OX}\left(\frac{W}{L}\right) \tag{3.5}$$

3.2.2 DIFFERENTIAL INTEGRATOR USING OTRA

The differential integrator circuit is shown in Fig. 3.4 with two resistors and a negative feedback capacitor [31]. The effect of stray capacitance is reduced by the virtual grounded connection of the feedback capacitor. The advantage of the proposed circuit is, it is possible to get both the positive and negative transfer function. The output voltage at terminal V_o can be given as

$$V_o = \frac{\omega_o}{s}(V_2 - V_1) \tag{3.6}$$

where

$$\omega_o = \frac{1}{RC} \tag{3.7}$$

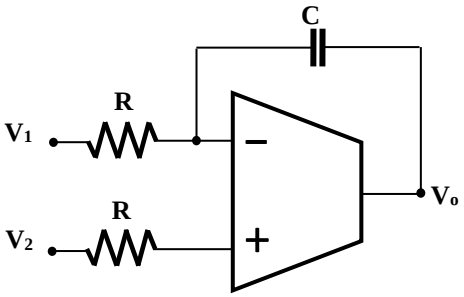

Fig. 3.4 Differential integrator using OTRA

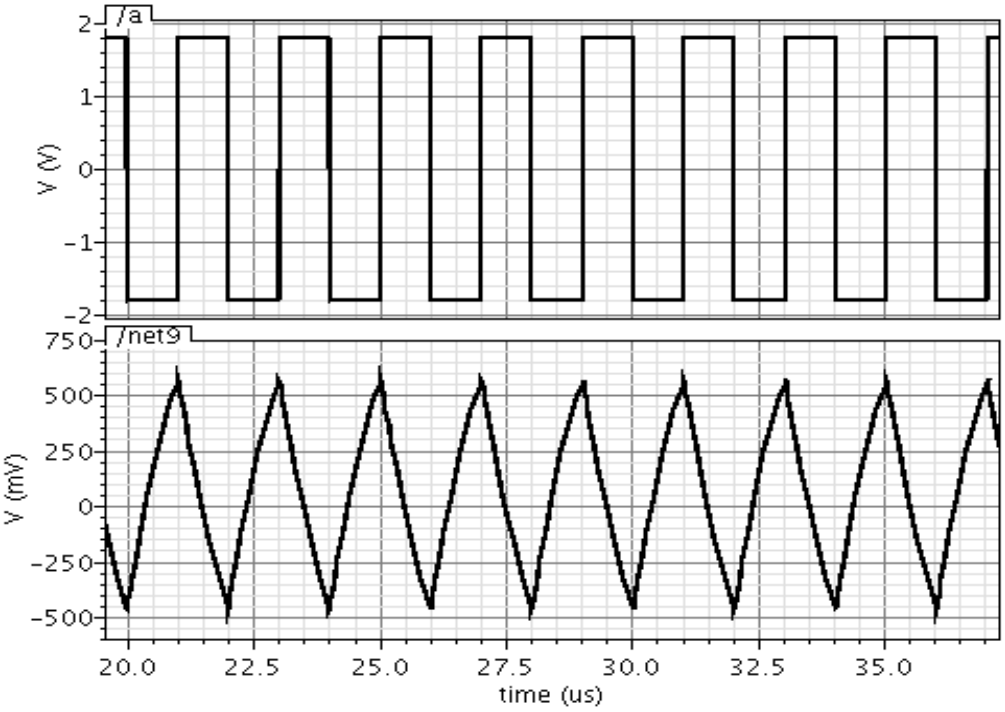

Fig. 3.5 Simulated output voltage of the differential integrator

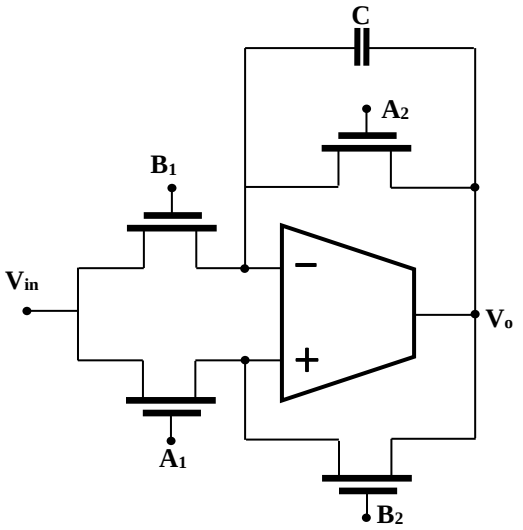

Fig. 3.6 Implementation of the OTRA differential integrator using MOS-C [31]

The transient response of the circuit in Fig. 3.4 is shown in Fig. 3.5. A feedback resistor is connected in parallel with the capacitor to solve the infinite gain problem in differential integrator circuit in Fig. 3.4. The advantage of connecting the capacitor in the feedback loop is to achieve the self compensation without any additional elements. The MOS-C implementation of the differential integrator using OTRA is shown in Fig. 3.6. The transfer function of the circuit in Fig. 3.6 is given by

$$\frac{V_o}{V_i} = \frac{G_1}{G_2} \frac{1}{\frac{s}{\omega_o} + 1} \tag{3.8}$$

Where

$$\omega_o = \frac{G_2}{C} \tag{3.9}$$

By adjusting the values of the gate voltages the differential integrator can achieve both ideal and lossy integration. The ideal integration can be done by making V_{A2} and $V_{B2} = 0$.

3.3 OTRA BASED SQUARE WAVEFORM GENERATORS

The first OTRA based square waveform generator was proposed by C. L. Hou *et al.*, [45] in the year 2005. In this work [45], two square waveform generators were proposed, these circuits consists of only one OTRA and a few external passive components.

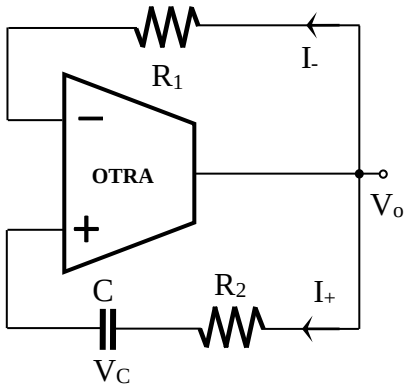

Fig. 3.7 OTRA based square waveform generator proposed in [45]

The first circuit was built with one OTRA and three passive components to produce the symmetrical square waveform with approximately fixed duty cycles and a variable frequency. The second circuit is able to control the on-duty and off-duty cycles of a square waveform independently by varying the value of the passive elements. This circuit was built with one OTRA, two diodes along with a few passive components. The first circuit with one OTRA and three passive components is shown in Fig. 3.7. The square waveform generators in [45] are simpler than the traditional voltage mode based (op-amp) waveform generators.

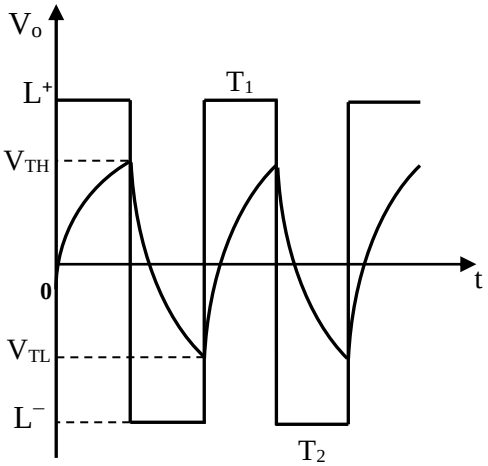

Fig. 3.8 Output waveform of the OTRA based square waveform generator in Fig. 3.7

The operation of the square waveform generator circuit in Fig. 3.7 can be explained with the help of its output waveform shown in Fig. 3.8. The output waveform in Fig. 3.8 has two saturation levels L^+ and L^-. Initially the output voltage V_o is at any one of these two saturation levels. The operation of the circuit can be explained as follows. Assume V_o is changing its state from L^- to L^+ at the time t = 0. At this time, the voltage V_C of the capacitor C starts to increase from its lower threshold value V_{TL} to its final value L^+. Where V_{TL} is the initial capacitor voltage at t = 0. In consequence, the capacitor voltage is finally charged to its upper threshold value V_{TH}, rather than L^+. When $t = T_1$, it also indicates that the current flowing into the non-inverting input terminal I_+ becomes slightly less than the inverting input terminal I_- current. So the output changes its state to the lower saturation level L^-. The upper threshold value and lower threshold value are derived from the non-inverting input terminal current I_+, inverting input terminal current I_- and from the ideal behaviour of OTRA is given in equations (3.10) and (3.11).

$$V_{TL} = \left(1 - \frac{R_2}{R_1}\right) L^- \tag{3.10}$$

$$V_{TH} = \left(1 - \frac{R_2}{R_1}\right) L^+ \tag{3.11}$$

Then the time period T_1 in Fig. 3.8 can be expressed as

$$T_1 = R_2 C \ln\left(\frac{V_{TL} - L^+}{V_{TH} - L^+}\right) \tag{3.12}$$

$$R_2 C \ln\left(\frac{2R_1}{R_2} - 1\right) = T_{on} \tag{3.13}$$

For time period T_2, the V_o remains at L^- and capacitor discharged until the non-inverting input terminal current I_+ becomes larger than inverting input terminal current I_-, when $V_C = V_{TL}$. The dynamic equation of V_C in the time period T_2 can be expressed as

$$T_2 - T_1 = R_2 C \ln\left(\frac{V_{TH} - L^-}{V_{TL} - L^-}\right) \tag{3.14}$$

$$R_2 C \ln\left(\frac{2R_1}{R_2} - 1\right) = T_{off} \tag{3.15}$$

From equations (3.14) and (3.15), for producing a square waveform in the circuit shown in Fig. 3.7, it is necessary that

$$R_1 > R_2 \tag{3.22}$$

The output square wave frequency f_o at the output terminal of the OTRA is given as

$$f_0 = \frac{1}{2R_2 C \ln\left(\frac{2R_1}{R_2} - 1\right)} \tag{3.23}$$

The on-duty and off-duty cycles of the square waveform for the Fig. 3.7 are almost fixed and it is not possible to increase or decrease the width of the duty cycles.

To eliminate this disadvantage, the second circuit was proposed in [45]. This circuit was designed with one OTRA, two diodes and four passive components. The second circuit is shown in Fig. 3.9.

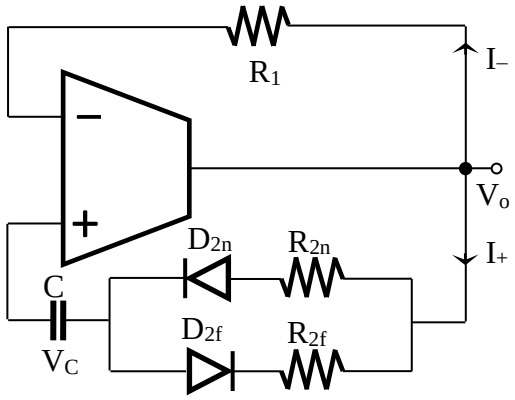

Fig. 3.9 Second proposed square waveform generator in [45]

The operation of the second proposed circuit in Fig. 3.9 is same as stated in the first proposed circuit operation. Neglecting the voltage drops of the diodes in the Fig. 3.9, the equations for the square waveform generator can be expressed as

$$T_{on} = R_2 C \ln\left(\frac{V_{TL} - L^+}{V_{TH} - L^+}\right) \tag{3.26}$$

$$R_{2n} C \ln\left(\frac{2R_1 - R_{2f}}{R_{2n}}\right) = T_{on} \tag{3.27}$$

$$T_{off} = R_{2f} C \ln\left(\frac{V_{TH} - L^-}{V_{TL} - L^-}\right) \tag{3.28}$$

$$R_{2f} C \ln\left(\frac{2R_1 - R_{2n}}{R_{2f}}\right) = T_{off} \tag{3.29}$$

$$f_o = \frac{1}{C\left(R_{2n} \ln\left(\frac{2R_1 - R_{2f}}{R_{2n}}\right) + R_{2f} \ln\left(\frac{2R_1 - R_{2n}}{R_{2f}}\right)\right)} \tag{3.30}$$

To produce a square waveform in the second proposed circuit, it is necessary to maintain

$$R_1 > R_{2n} \tag{3.31}$$

and

$$R_1 > R_{2f} \tag{3.32}$$

The on-duty (T_{on}) and off-duty (T_{off}) cycles can be varied independently by adjusting R_{2n} and R_{2f} respectively.

3.3.1 SIMULATION RESULTS

For designing the fixed duty cycle circuit shown in Fig. 3.7, the operating frequency f_o is chosen first. Then the value of resistors R_1 and R_2 is chosen. The ratio of R_1/R_2 is chosen as low as possible. The larger R_1/R_2 ratio results in a less sensitivity of the frequency variation with respect to the resistance. The capacitor value is arbitrarily chosen from the equation (3.23).

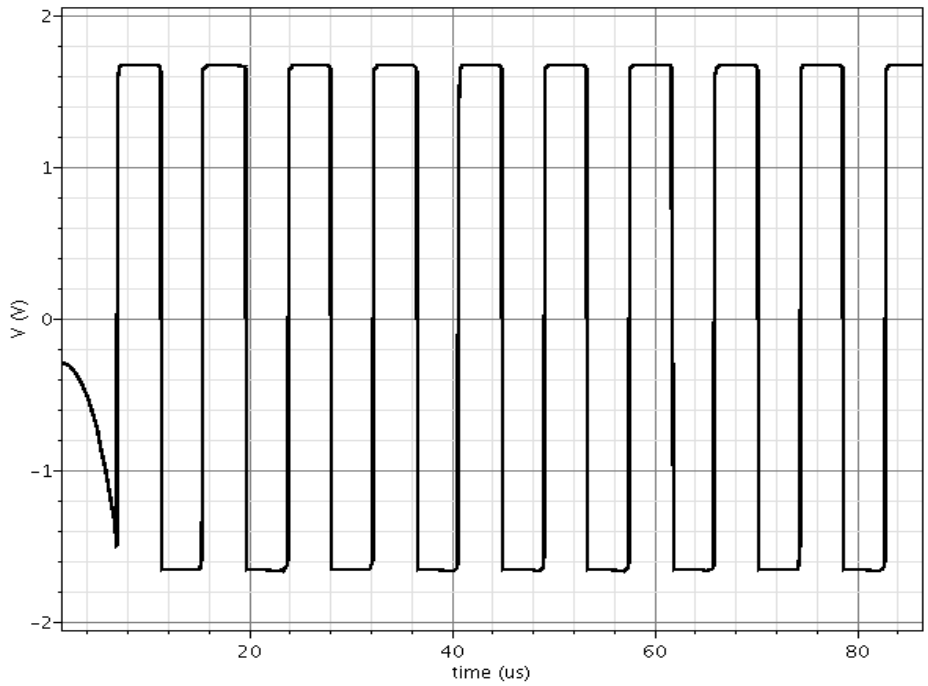

Fig. 3.10 Simulation result of the square waveform generator circuit in Fig. 3.7

For example, if f_o is chosen as 100 kHz, then the ratio of resistors R_1/R_2 is set to be 10 and C is arbitrarily chosen as 1nF. Then R_2 and R_1 can be calculated from equation (3.23) as 1.7 kΩ and 17 kΩ. If the required frequency is 100 Hz, then 1 nF capacitor is replaced by 1 µF capacitor without changing the R_1/R_2 ratio. In order to investigate the circuits proposed in [45], several experiments were performed on circuits shown in Fig. 3.7 and Fig. 3.9 at supply voltages ± 1.8 V. The Cadence Spectre simulation result for the proposed circuit in Fig. 3.7 is shown in Fig. 3.10 with

a frequency of 100 kHz. The passive components R_1 = 17 kΩ, R_2 = 1.7 kΩ and C = 1 nF were used for the simulation. For selecting the passive component values for the second circuit shown in Fig. 3.9, followed the same procedure as stated to select the passive component values in the first square waveform generator circuit. For example, if f_o is chosen as 100 kHz, the circuit parameters are selected as C = 1nF, R_1 = 17 kΩ, and $R_2 = R_{2f} = R_{2n}$ = 1.7 kΩ. The simulated output waveform for the circuit in Fig. 3.9 is shown in Fig. 3.11.

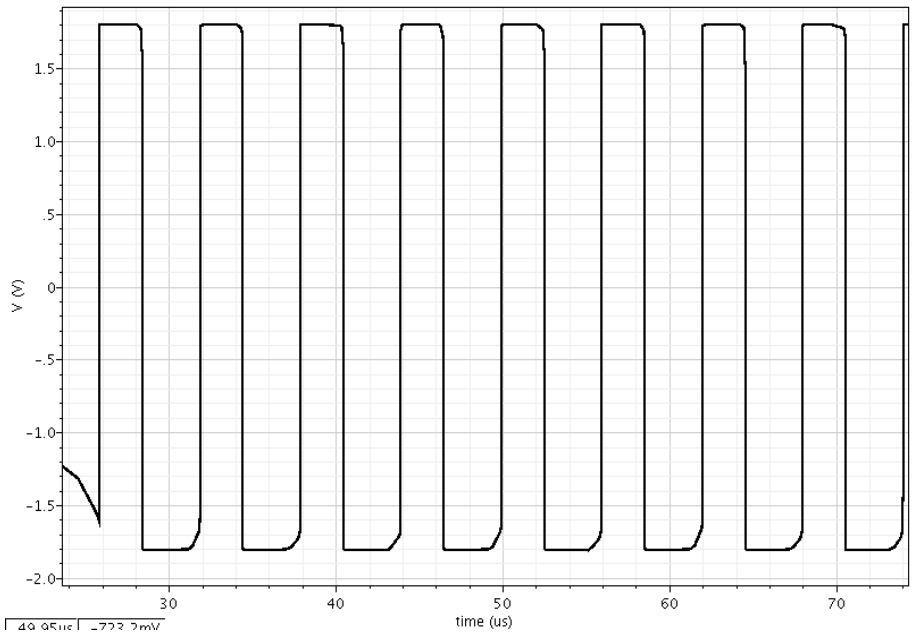

Fig. 3.11 Simulation result of the square waveform generator circuit in Fig. 3.9

The resistors R_{2f} and R_{2n} are varied independently to vary the on-duty and off-duty cycles of the output square waveform.

3.3.2 DISCUSSIONS AND CONCLUSIONS

The proposed circuits in [45] are simpler than the traditional voltage-mode square waveform generators. From Fig. 3.10, it can be seen that the on-duty and off-duty cycles are not same for the first proposed circuit in Fig. 3.7. Small percentage of error present between the on-duty and off-duty cycles. For the second circuit shown in Fig. 3.9, the capacitor value is slightly adjusted to fine tune the output square wave frequency. For the 60% on-duty cycle, R_{2n} is larger than the R_{2f}. The capacitor voltage increases to a smaller V_{TH} with an even slower charging rate in the on-period. The minimum frequency range of the square waveform circuits in Fig. 3.7 and 3.8 is

limited by the values of the passive components connected to the circuits, mainly the capacitor. Large value of capacitor makes lower output frequency.

The highest frequency at the output terminal is limited due to the slew-rate of the active device. The highest output frequency is around several MHz. However, the circuit has the advantage of less passive components, but it makes a non-linear variation of the time period with respect to the resistor R_2 and R_1 value sholud be larger than R_2 value to produce oscillations. The Fig. 3.12 shows the non-linear variation of time period with respect to the resistor R_2. For tuning the resistor R_2, passive components C = 1nF R_1 = 18kΩ were chosen and R_2 was varied from 200Ω to 18 kΩ. Moreover, the circuits proposed in [45] consume large amount of power with a supply voltage of ± 15 V.

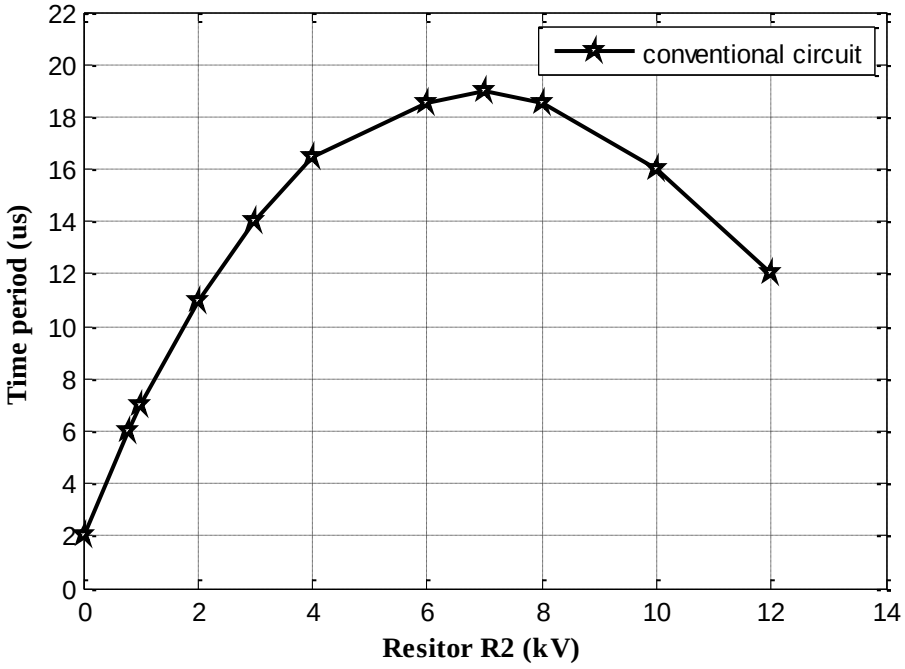

Fig. 3.12 Variation of time period for the square waveform generator circuit shown in Fig. 3.9

3.4 OTRA BASED SQUARE/TRIANGULAR WAVEFORM GENERATOR

The OTRA based square/triangle waveform generator was proposed by Y. K. Lo *et al.,* in the year 2007 [46]. The circuit was implemented with two OTRAs, three switches and a few passive components. The circuit proposed in [46] has an advantage of producing both inverting and non-inverting mode of operations. The OTRA based square/triangle waveform generator is shown in Fig. 3.13. The operation

of the circuit can be explained as follows: for inverting mode operation the switches a2 is connected to c2 and a3 is connected to b3. For non-inverting mode operation the switches are connected as; a2 is connected b2 and a3 is connected to c3. The expected output waveform is shown in Fig. 3.14.

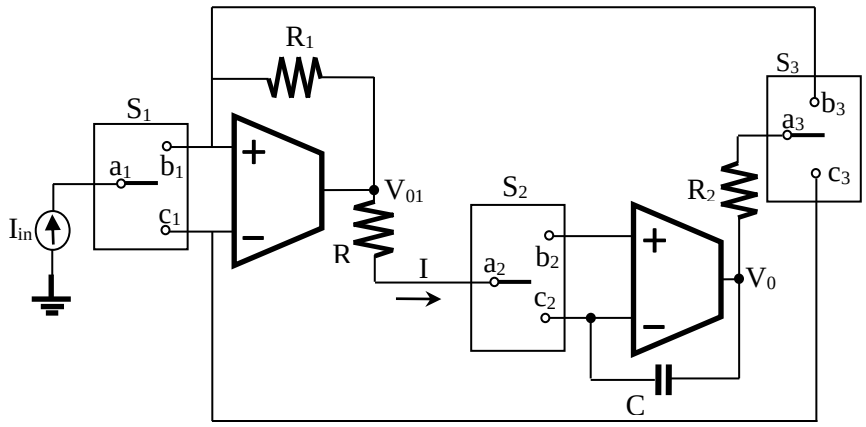

Fig. 3.13 OTRA based square/triangle waveform generator

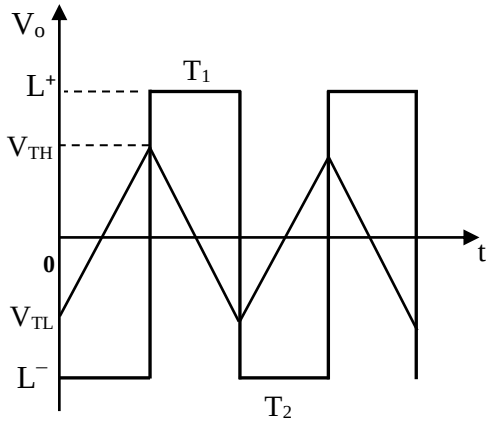

Fig. 3.14 Expected output waveform from the circuit in Fig. 3.13

From the Fig. 3.14, the output is at negative saturation level L^-. The saturation current I, flows through the resistor R and C, this makes V_{02} to increase linearly.

$$I = \frac{V_{01}(t)}{R} = \frac{L^-}{R} = C\frac{dV_{02}}{dt} \tag{3.33}$$

This state continues until V_{02} reaches the upper threshold voltages $V_{TH.}$ The upper threshold voltage can be derived by making inverting and non-inverting currents equal.

$$V_{TH} = R_2 I_{in} + \frac{R_2}{R_1} L^+ \tag{3.34}$$

When a1 is connected to b1,

$$V_{TH} = -R_2 I_{in} + \frac{R_2}{R_1} L^+ \tag{3.35}$$

Similarly, for lower threshold voltage V_{TL},

$$V_{TL} = R_2 I_{in} - \frac{R_2}{R_1} L^+ \tag{3.36}$$

$$V_{TL} = -R_2 I_{in} - \frac{R_2}{R_1} L^+ \tag{3.37}$$

The on-duty and off-duty cycles time period can be derived from the equations (3.34)-(3.37).

$$T_1 = 2RC \frac{R_2}{R_1} \tag{3.38}$$

and for off-duty cycle,

$$T_2 = 2RC \frac{R_2}{R_1} = T_{off} \tag{3.39}$$

The oscillation frequency is given by,

$$f = \frac{1}{4RC\left(\frac{R_2}{R_1}\right)} \tag{3.40}$$

3.4.1 SIMULATION RESULTS

The circuit shown in Fig. 3.13 was simulated using Cadence Spectre simulation model parameters. The simulated square/triangular waveform is shown in Fig. 3.15.

3.4.2 DISCUSSIONS AND CONCLUSIONS

The equation (3.40) is useful to facilitate the design of square/triangular waveform generator shown in Fig. 3.13. The oscillation frequency is specified first, and then the ratio R_2/R_1 is found from equation (3.40) for an arbitrarily chosen capacitor C and resistor R values. The circuit has an advantage of producing both inverting and non-inverting output waveforms. The circuit presented in [46] is

successfully eliminated the errors presented in voltage-mode square/triangle waveform generator, specifically frequency and amplitude are dependent.

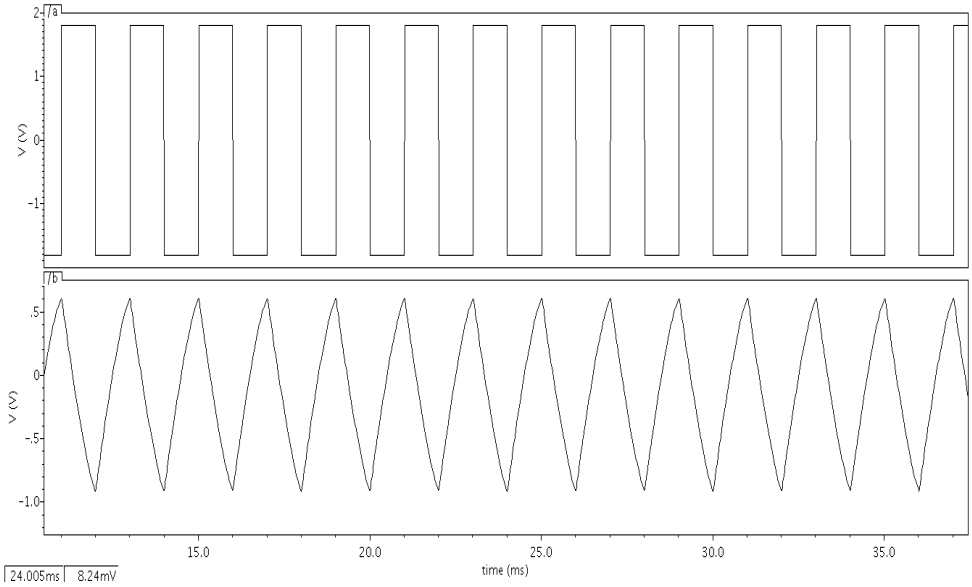

Fig. 3.15 Simulated output waveform from the circuit in Fig. 3.13

The minimum and maximum frequency range of the circuit is from kHz to few MHz. The minimum frequency is limited by the capacitor value and the maximum frequency is limited by the slew rate of the OTRA. However, the circuit shown in Fig. 3.13 is complex with three switches, two OTRAs and four passive components. Moreover, the circuit requires external current source I to adjust the DC level of the output waveform. The operation of the circuit is also complex with the switching positions of three switches. The circuit consume high power to operate with two OTRAs, three switches and four passive components.

3.5 OTRA BASED SINUSOIDAL OSCILLATORS

The first OTRA based sinusoidal waveform generator was proposed by K. N. Salama *et al.,* in the year 2000 [50]. Seven new sinusoidal oscillator designs are reported in [50]. In this paper, three oscillator circuits are realized from a generalized configuration using single OTRA and four sinusoidal oscillator circuits are designed using two OTRAs with a few passive components. The generalized configuration to realise several sinusoidal oscillators using single OTRA is shown in Fig. 3.16.

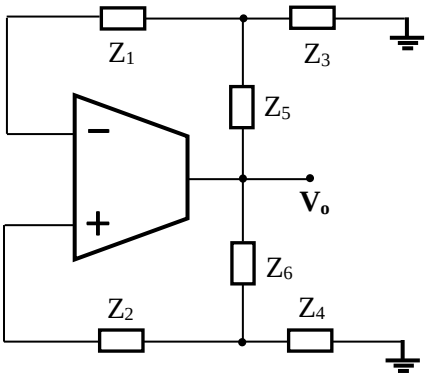

Fig. 3.16 OTRA based generalized configuration.

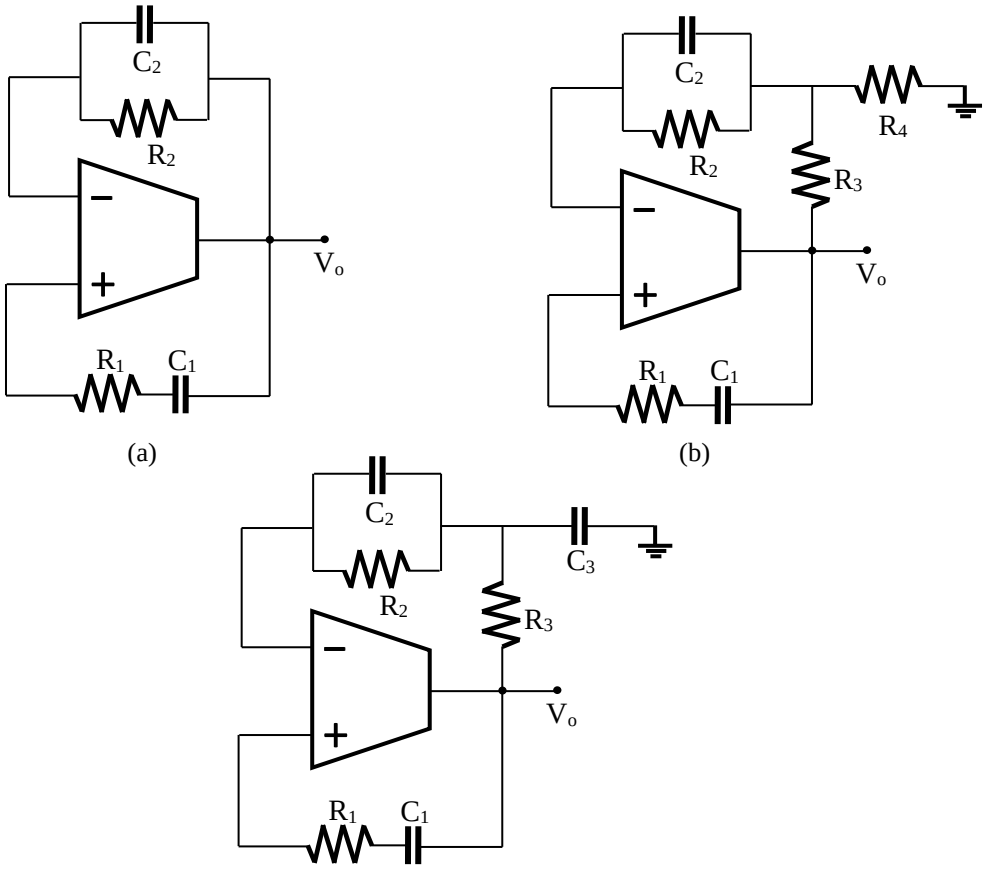

Fig. 3.17 Oscillators realized from the generalized configuration in Fig. 3.16

Assuming the OTRA used in the generalized configuration is ideal; the characteristic equation for the generalized configuration is by:

$$Z_2 + Z_5\left(1+\frac{Z_2}{Z_3}\right) = Z_1 + Z_6\left(1+\frac{Z_1}{Z_4}\right) \tag{3.41}$$

Several oscillator circuits can be realized from the generalized configuration. Three special cases are shown in the Fig. 3.17. Minimum passive component oscillator that can be realized from the generalized configuration is show in Fig. 3.17 (a). The circuit shown in Fig. 3.17 (a) requires two capacitors and two resistors to produce the oscillation. The condition of oscillation and frequency of oscillation are given by

$$\frac{R_1}{R_2}+\frac{C_2}{C_1}=1 \tag{3.42}$$

$$\omega_o=\frac{1}{\sqrt{C_1C_2R_1R_2}} \tag{3.43}$$

From equations (3.42) and (3.43), it is clear that the condition of oscillation and frequency of oscillation cannot be controlled independently from the circuit in Fig. 3.17 (a). The oscillator circuits shown in Fig. 3.17 (b) & (c) are able to control the condition of oscillation and frequency of oscillation independently. The characteristic equations for the circuits shown in Fig. 3.17 (b) & (c) can be derived from the generalized equation (3.41). For the oscillator circuit in Fig. 3.17 (b), the grounded resistor R_4 is used to control the condition of oscillation without affecting the frequency of oscillation. From the equations (3.46) and (3.47), the capacitor C_3 in Fig. 3.17 (c) is used to control the frequency without affecting the condition of oscillation. Four quadrature oscillators using two OTRAs are shown in Fig. 3.18 [50].

For Fig. 3.17 (b)

$$\frac{R_1}{R_2}+\frac{C_2}{C_1}=1+\frac{R_3}{R_2}+\frac{R_3}{R_4} \tag{3.44}$$

$$\omega_o=\frac{1}{\sqrt{C_1C_2R_1R_2\left(1-\frac{R_3}{R_1}\right)}} \tag{3.45}$$

For Fig. 3.17(c)

$$\frac{R_1}{R_2}+\frac{C_2}{C_1}=1+\frac{R_3}{R_2} \tag{3.46}$$

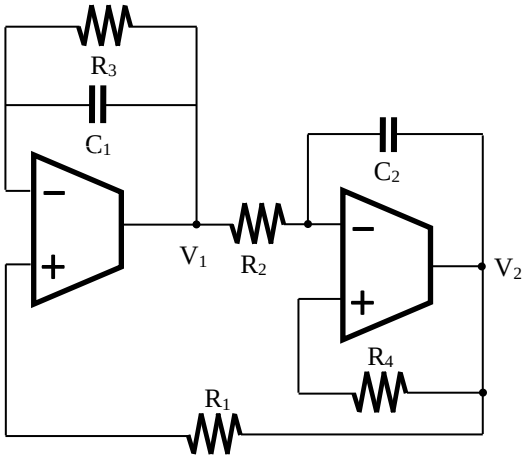

(a)

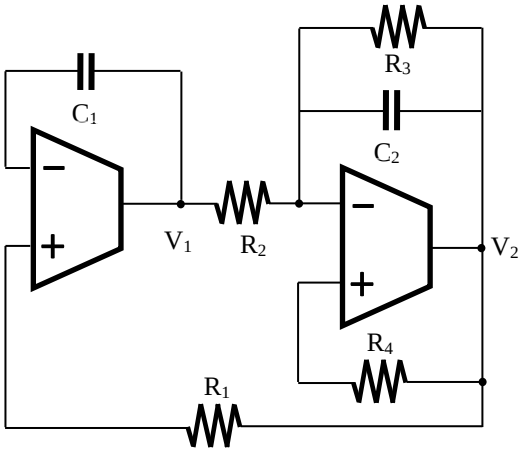

(b)

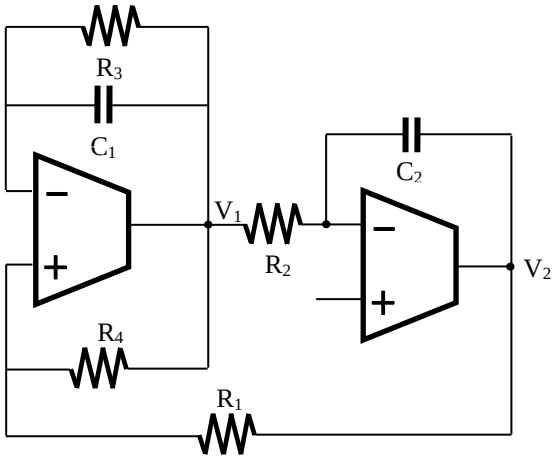

(c)

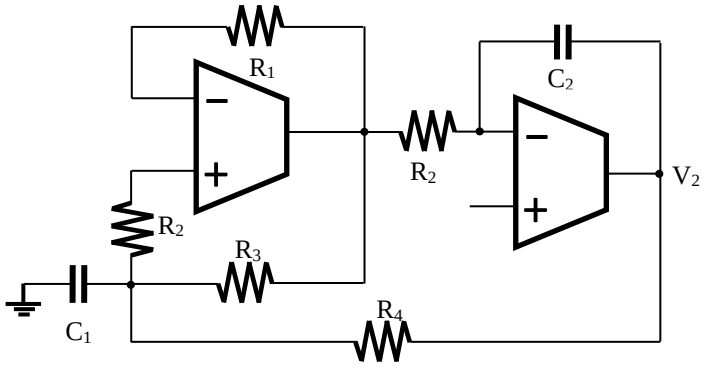

(d)

Fig. 3.18 Sinusoidal oscillators using two OTRAs

$$\omega_o = \frac{1}{\sqrt{C_1 C_2 R_1 R_2 \left(1 - \frac{R_3}{R_1}\left(1 + \frac{C_3}{C_2}\right)\right)}} \tag{3.47}$$

These oscillator circuits are constructed with two capacitors and four or five resistors. All the circuits shown in Fig. 3.18 are able to control the frequency of oscillation and condition of oscillation independently. The condition of oscillation and frequency of oscillation for these circuits are derived from the state matrix of the corresponding circuits.

$$C_1 R_3 = C_2 R_4 \tag{3.48}$$

$$\omega_o = \frac{1}{\sqrt{C_1 C_2 R_1 R_2 \left(1 - \frac{R_1 R_2}{R_3 R_4}\right)}} \tag{3.49}$$

The equations (3.48) and (3.49) are derived from the state matrix shown below for the circuit in Fig. 3.18 (a).

$$\begin{bmatrix} \frac{dV_1}{dt} \\ \frac{dV_2}{dt} \end{bmatrix} = \begin{bmatrix} -\frac{1}{C_1 R_3} & \frac{1}{C_1 R_1} \\ -\frac{C_2}{R_2} & \frac{1}{C_2 R_4} \end{bmatrix} \begin{bmatrix} V_1 \\ V_2 \end{bmatrix} \tag{3.50}$$

The condition of oscillation and frequency of oscillation is same for the circuits in Figs. 3.18 (b) and (c).

$$R_3 = R_4 \tag{3.51}$$

$$\omega_o = \frac{1}{\sqrt{C_1 C_2 R_1 R_2}} \tag{3.52}$$

For producing oscillations in the circuit shown in Fig. 3.18 (d), it requires, two OTRAs, four resistors and two capacitors. The condition of oscillation and frequency of oscillation is given in equations (3.53) and (3.54).

$$R_3 = 3R \tag{3.53}$$

$$\omega_o = \frac{3}{\sqrt{C_1 C_2 R_1 R_2}} \tag{3.54}$$

A novel single resistance controlled sinusoidal oscillator employing single OTRA was proposed by U. Cam in the year 2002 [51]. The circuit proposed in [51] is simpler than the circuits in Fig. 3.17.

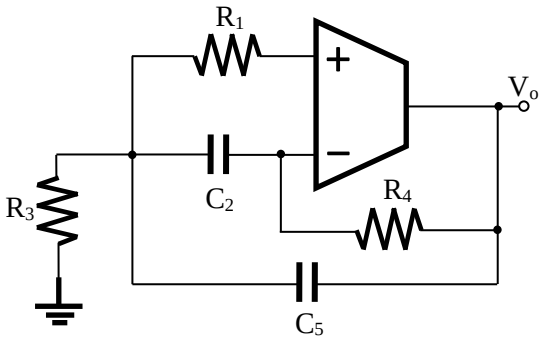

Fig. 3.19 SRCO using single OTRA

The circuit diagram of the oscillator is shown in Fig. 3.19. Routine analysis for the above circuit gives the following equations.

$$C_2G_4 + C_5G_4 = C_5G_1 \tag{3.55}$$

$$f = \frac{1}{2\pi}\sqrt{\frac{G_4(G_1+G_3)}{C_2C_5}} \tag{3.56}$$

Form the above equations (3.55) and (3.56), it is clear that the grounded resistor R_3 is used to control the frequency of the oscillator without disturbing the condition of oscillation. This oscillator is also called as single resistance controlled oscillator (SRCO). Minimum component oscillator along with one SRCO and one single capacitance controlled oscillator (SCCO) were proposed in [52]. The circuits reported in [52] are shown in Fig. 3.20. The minimum component oscillator is shown in Fig. 3.20 (a). This oscillator circuit requires two capacitors and two resistors to produce the oscillation. However, it is not possible to control the condition of oscillation and frequency of oscillation independently with the minimum component circuit in Fig. 3.20 (a). The mathematical equations derived from the above circuits are given in the below equations. For Fig. 3.20 (a)

$$\frac{G_2}{G_1} - 1 = \frac{C_2}{C_1} \tag{3.57}$$

$$\omega_o = \sqrt{\frac{G_1 G_2}{C_1 C_2}} \tag{3.58}$$

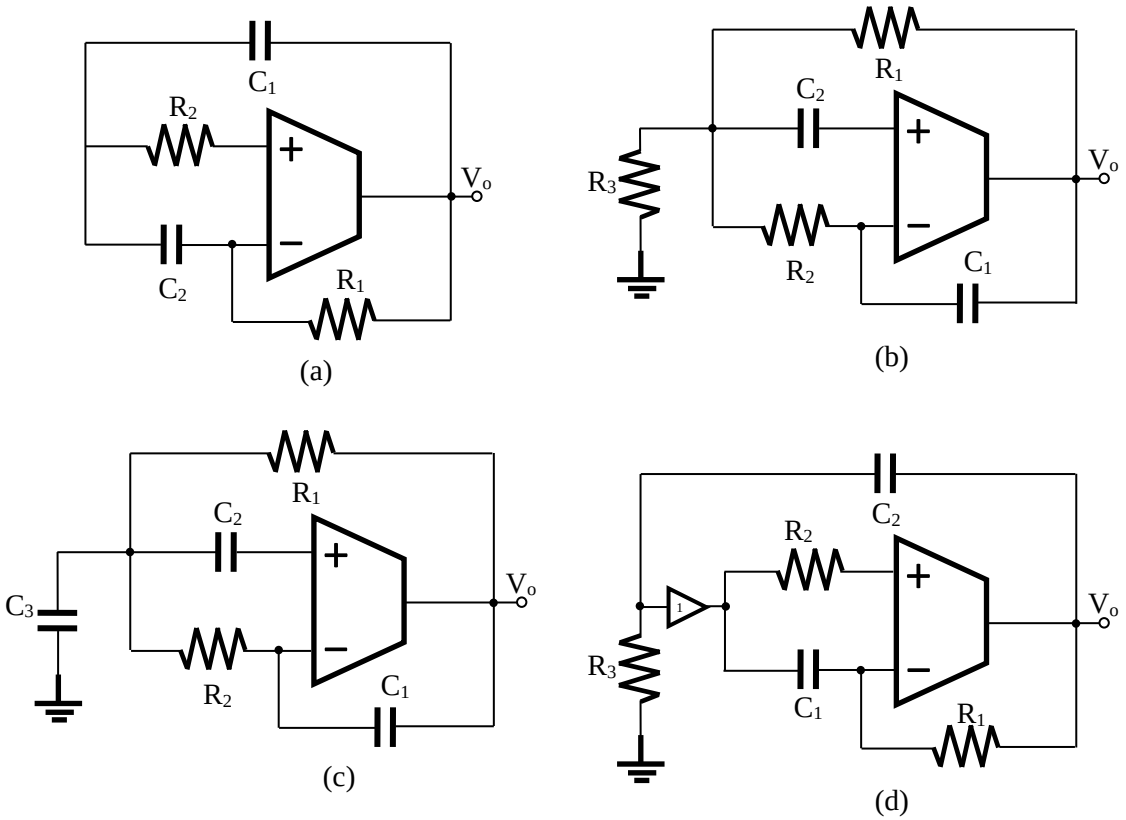

Fig. 3.20 Minimum component, SRCO and SCCO oscillators using single OTRA

For Fig. 3.20 (b)

$$1 + \frac{G_2}{G_1} + \frac{G_3}{G_1} = \frac{C_2}{C_1} \tag{3.59}$$

$$\omega_o = \sqrt{\frac{G_1 G_2}{C_1 C_2}} \tag{3.60}$$

For Fig. 3.20 (c)

$$1 + \frac{G_2}{G_1} = \frac{C_2}{C_1} \tag{3.61}$$

$$\omega_o = \sqrt{\frac{G_1 G_2}{C_1 (C_2 + C_3)}} \tag{3.62}$$

The oscillator circuits shown in Fig. 3.20 (b) & (c) are able to control the oscillation condition and the frequency of oscillation independently and the same is proven from the equations (3.59)-(3.62). The circuit shown in Fig. 3.20 (d) was proposed by Ashish G. *et al.*, in the year 2012 [53]. Two grounded resistance/capacitance (SRCO/SCCO) oscillators were reported in [53], the first oscillator circuit [53] with a grounded capacitor is similar to the circuit shown in Fig. 3.19 (c). These oscillator circuits can also be used as grounded inductance simulators by removing the grounded passive components and applying input current to the buffer. The condition of oscillation and frequency of oscillation derived from the circuit in Fig. 3.19 (d) is given in equations (3.63) and (3.64).

$$R_2 \leq R_1 \tag{3.63}$$

$$f = \frac{1}{2\pi\sqrt{R_1 R_3 C_1 C_2}} \tag{3.64}$$

3.5.1 SIMULATION RESULTS

All the circuits shown in Figs. 3.17, 3.18, 3.19 and 3.20 were simulated using Cadence Spectre simulation model parameters. The simulation result for the circuit in Fig. 3.17 (a) is shown in Fig. 3.21. The passive components R_1 =10 kΩ, R_2 = 20 kΩ, C_1 =10 nF and C_2 =15 nF were used for the simulation with a supply voltage of ± 1.8 V.

3.5.2 DISCUSSIONS AND CONCLUSIONS

The oscillator circuits shown Figs 3.17, 3.18, 3.19 and 3.20 are able to produce sinusoidal waveforms from a few kHz to several MHz. The circuits shown in Fig. 3.17 (a) and 3.20 (a) are minimum component oscillators. The advantages of these two circuits are less in number of passive components and single OTRA. However, all the passive components used in these two circuits are floating and it is hard to fabricate the integrated circuit (IC) with all floating passive components. The generalized configuration shown in Fig. 3.16 is used to realize only few oscillator circuits. The frequency spectrum is also given for the circuit in Fig. 3.17 (a). The oscillator circuits generated from the generalized configuration require more number of passive components. The oscillator circuits realized from the generalized configuration are shown in Fig. 3.17 (b) & (c).

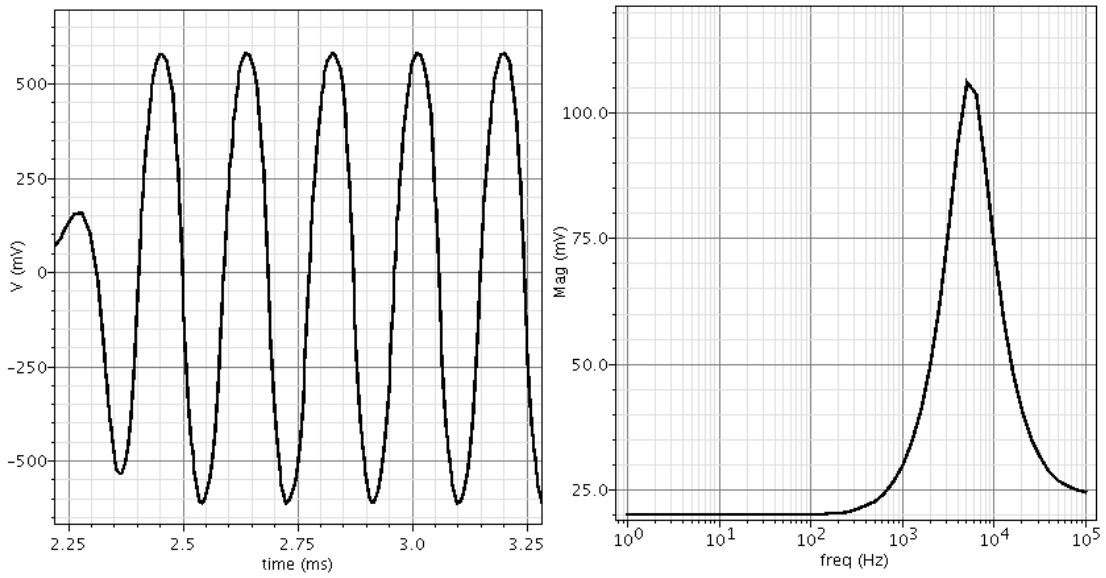

Fig. 3.21 Simulation result for the oscillator circuit shown in Fig. 3.17 (a)

These two oscillator circuits require six passive components to generate the oscillations. However, these circuits have grounded passive components, but, more passive component occupies greater chip area in IC fabrication. The oscillator circuits shown in Figs. 3.18(a), (b) and (c) are quadrature sinusoidal oscillators. These quadrature oscillators produce two sinusoidal outputs with 90^o phase difference between them. The oscillator circuit shown Fig. 3.18 (d) requires two OTRAs and seven passive components. This oscillator circuit consumes high power to produce the oscillation. A similar circuit with two OTRAs and three resistors and three capacitors is reported in [64]. This circuit also consumes a high amount of power to produce the oscillations.

3.6 SUMMARY

A brief on existing OTRA based waveform generators available in the literature is presented in this chapter. The circuits given in this chapter are redesigned using Cadence gpdk 180 nm and simulated using Spectre simulation model parameters. A few OTRA applications are also included in this chapter. The working of OTRA based circuits such as sinusoidal oscillators, square waveform generators and square/triangular waveform generator is given in brief. The disadvantages detected during the simulation and hardware implementation of the existing OTRA based circuits are presented as intermediate conclusions in the subtopics of this chapter.